Searches for new resonances

La Thuile 2024

Noam Tal Hod, on behalf of ATLAS and CMS

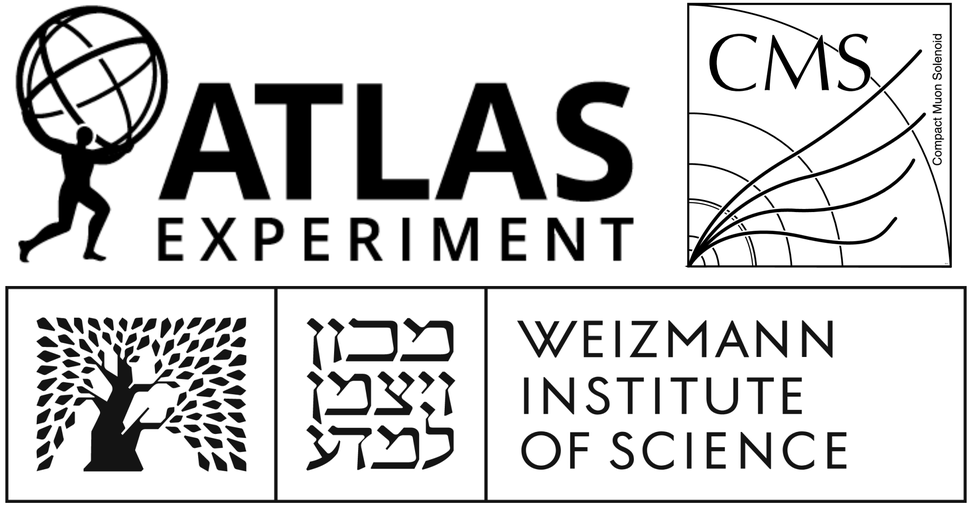

Introduction

- Majority of BSM theories predict new heavy particles
- Many searches over the years, ~thousands just at the LHC (>15 years!)
- Access to new resonances up to $\mathcal{O}(100)$ times the EW scale!
- For a nice review of the experimental status, see arXiv:2311.09824

This talk:

- Highlighting latest ATLAS & CMS searches for new resonances
- Not delving into selections etc., but only highlighting the uniquenesses
- Focusing on the experimental signatures rather than on specific models

ATLAS

Click the title for the full list of ATLAS results

Since ~Jul 2023

CMS

Click the title for the full list of CMS results

Definitely

- High mass resonances in τ+MET (Feb 2024)
- Heavy resonances with 4l+MET/jets (Jan 2024)
- Resonances w/pairs of merged diphotons (Dec 2023)
- Narrow trijet resonances (Oct 2023)

Maybe

- Combination of heavy resonances (Feb 2024)
- Combination of HH resonances (Nov 2023)

Not

- Dark jets (Nov 2023)
- W'→tb 0/1-lepton (Aug 2023)
- Paired dijet resonances (Jul 2023)
- Resonant SH to VVtautau (Jul 2023)
- LFV Z' → emu, etau, mutau (Jul 2023)
- W'→tb in leptonic final states (Oct 2023)
- GeV-scale resonances w/pair of muons (Sep 2023)
- Data scouting w/pairs of multijet resonances (Aug 2023)
- High-mass dimuon resonances w/b-jets (Jul 2023)
- Z' to pairs of heavy Majorana neutrinos (Jul 2023)

τ_{had}+MET 2402.16576

- Looking at W' within the SSM and on Non-Universal Gauge Interaction Models
  - $\tan\theta_{NU}$ scales the couplings to the 1st/2nd gen. fermions,
  - $\cot\theta_{NU}$ scales the couplings to the 3rd gen.
    - SSM for =1, enhanced 3rd gen for >1
  - Width is $\sim 3\% - 36\%$ ($W' \to WZ/Wh$ decays neglected)
  - Model-dependent interference between W and W' is <u>not</u> considered

- Using hadronic τ's, which <u>include a ν</u> and a set of visible products $\tau_{had-vis}$
  - typically $1/3\pi^{\pm}$ and $\leq 2\pi_0$

- Backgrounds:
  - From MC: $W \to \tau\nu$ (and other backgrounds)
  - From data: W/Z + jets, $Z(\to \nu\nu)$ + jets and Multijet
    - Taus failing the SR τ-ID, transferred w/factors measured in CRs

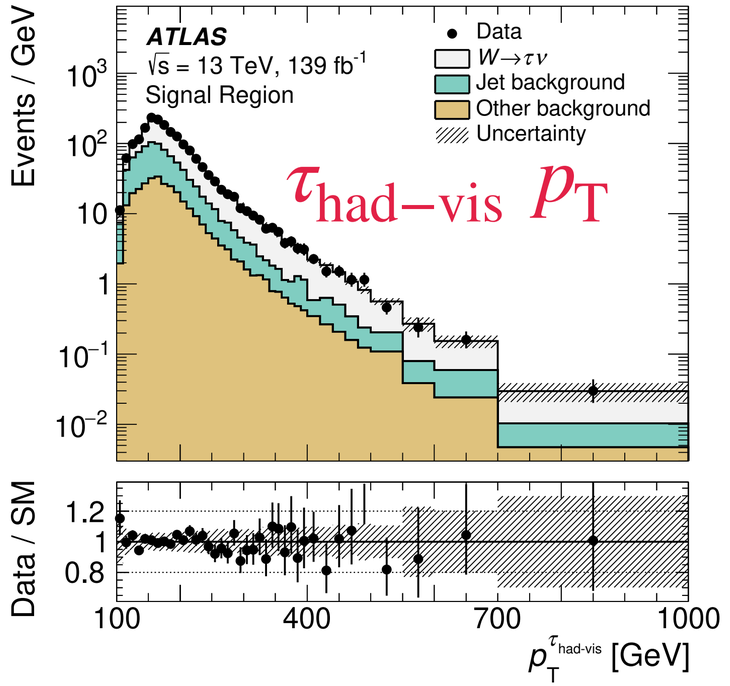

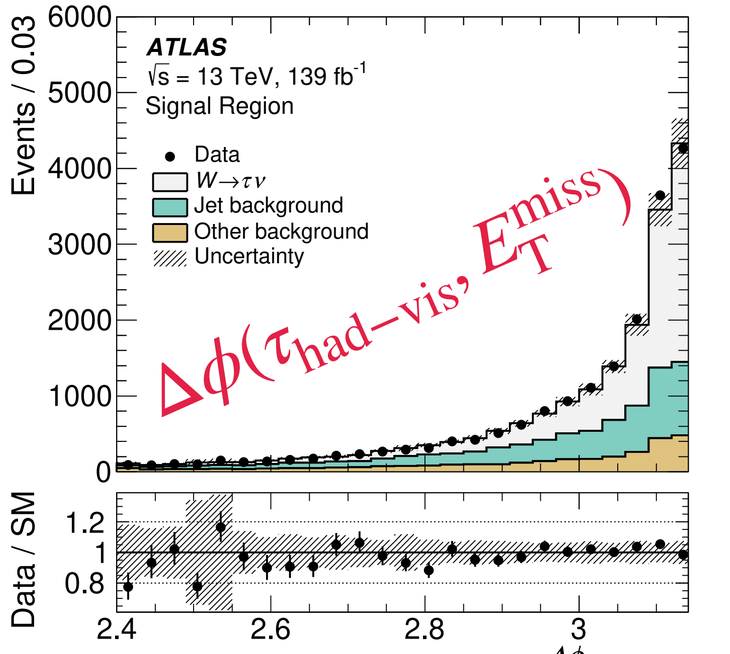

τ_{had}+MET 2402.16576

- Charged tracks within $\Delta R < 0.2$ around the $\tau_{\text{had-vis}}$ are associated using a BDT
  - better efficiency at high p_T wrt the past
- RNN τ identification (ATL-PHYS-PUB-2019-033)
  - efficiency: 85%(75%) for 1(3)-prongs
- e-rejection BDT (ATLAS-CONF-2017-029)
  - for 1-prong τ's efficiency of 95%
- SR: $E_T^{miss} > 150$ GeV, $\Delta\phi > 2.4$, and $0.7 < \frac{p_T}{E_T^{miss}} < 1.3$

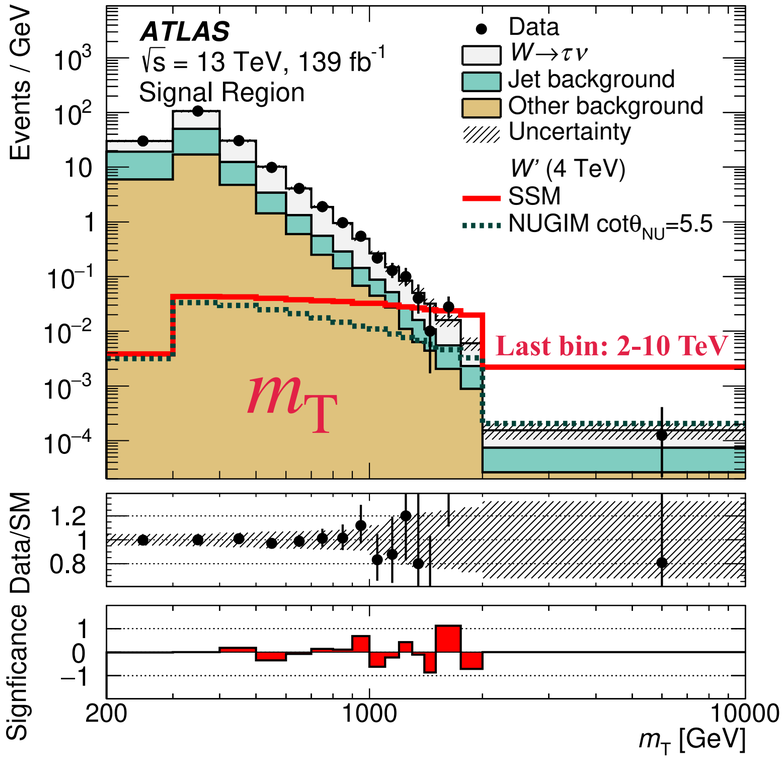

Improvements wrt 36 fb^{-1}
- multi-bin search,
- improved τ-ID,
- track-to-τ assoc. BDT

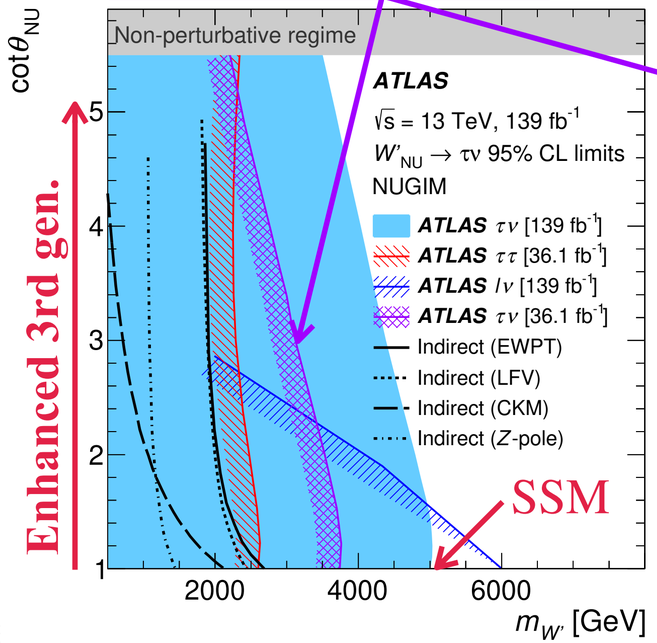

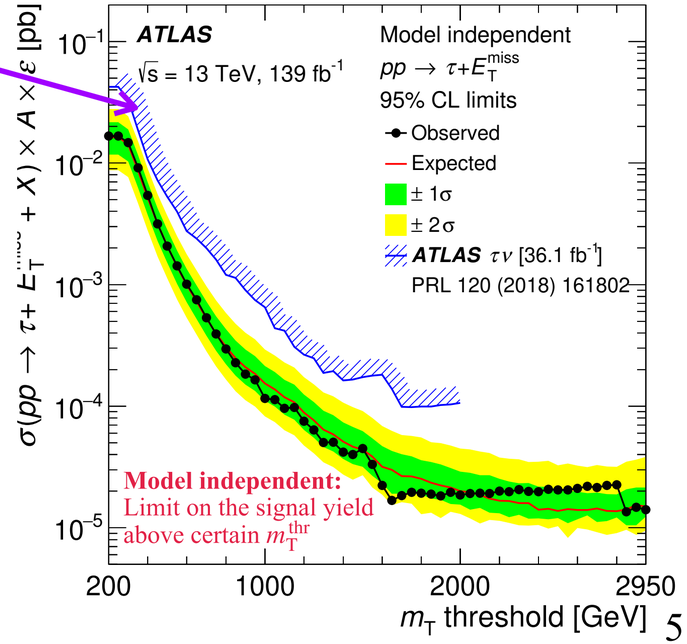

Highly merged $\gamma\gamma$ pairs EXO-22-022

- Extended Higgs sectors with $X \to \phi\phi \to \gamma\gamma + \gamma\gamma$
  - $0.5\,\% < m_\phi/m_X < 2.5\,\%$ $(200 \lesssim \phi$ boost $\lesssim 14)$
  - $\phi \to \gamma\gamma$ can happen via (B)SM loops
  - $\phi \to b\bar{b}$ early search is limited to $m_\phi > 2m_b$

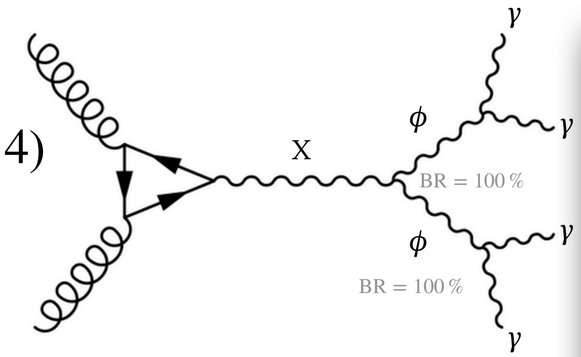

- Pairs **($\Gamma \equiv \gamma\gamma$)** reconstructed in the EMCAL barrel
  - 61,200 crystals, covering $\Delta\eta \times \Delta\phi = 0.0175^2$ each
  - Deposits of one Γ are abstracted as a pixelated image
- Use two CNNs to identify and characterize the Γ's
  - CNN_1 separates from bkg Γ's produced by hadrons / single photons
  - CNN_2 regresses the mass-to-energy ratio (m/E) of a given Γ
  - Performance is validated on $Z \to ee$ and $\eta \to \gamma\gamma$ events
- Search for excess in $m_{\Gamma\Gamma}$, in 9 slices of $0.3 < \alpha \equiv \hat{m}_\Gamma/m_{\Gamma\Gamma} < 3\,\%$ $\to$ $\alpha \sim m_\phi/m_X$
  - Background is modeled from a fit to the data per slice

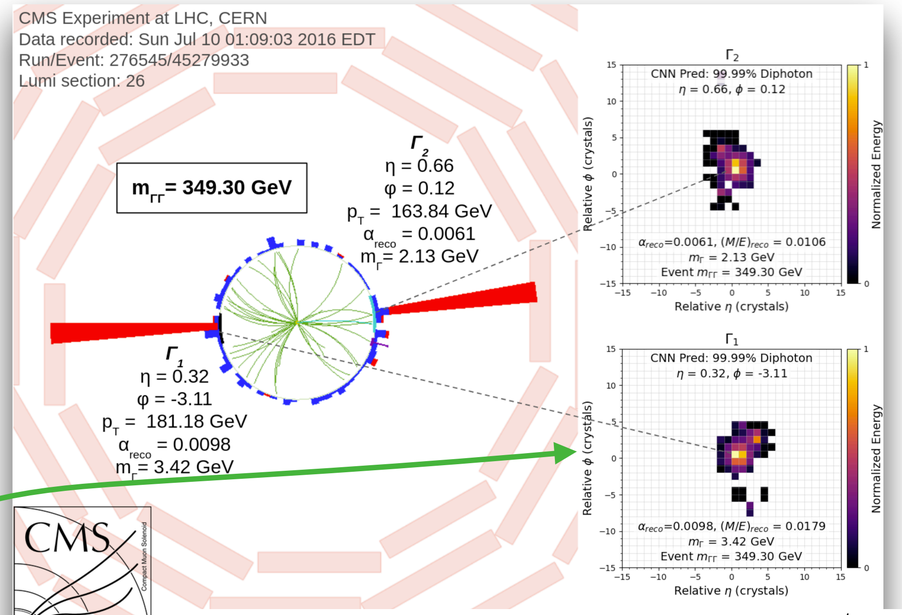

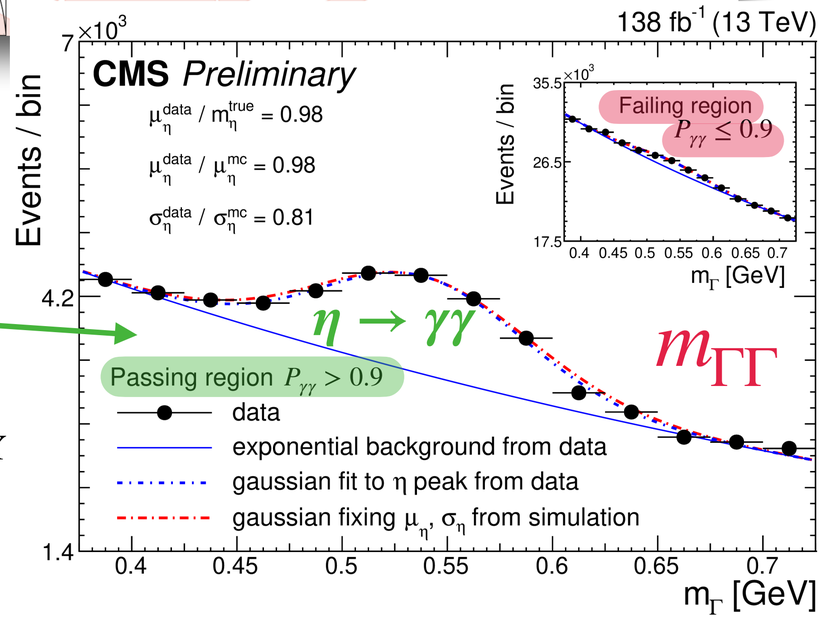

Highly merged $\gamma\gamma$ pairs EXO-22-022

- Background uncertainties: function choice and its fit parameters
- Signal uncertainties: diphoton classifier efficiency (10%, per cluster)
- LH fit is done simultaneously in all 9 slices of α
- $\sigma(X \to \phi\phi \to 4\gamma) \propto N_q m_X/f$: N_q is the number of quark flavors receiving all their mass from the $X_{\mathrm{VEV}} = f$

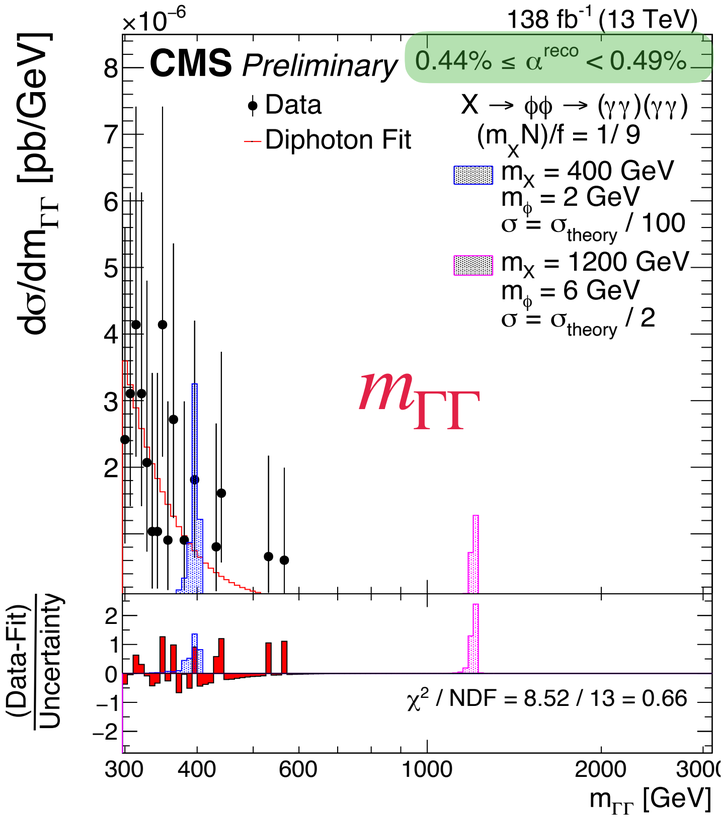

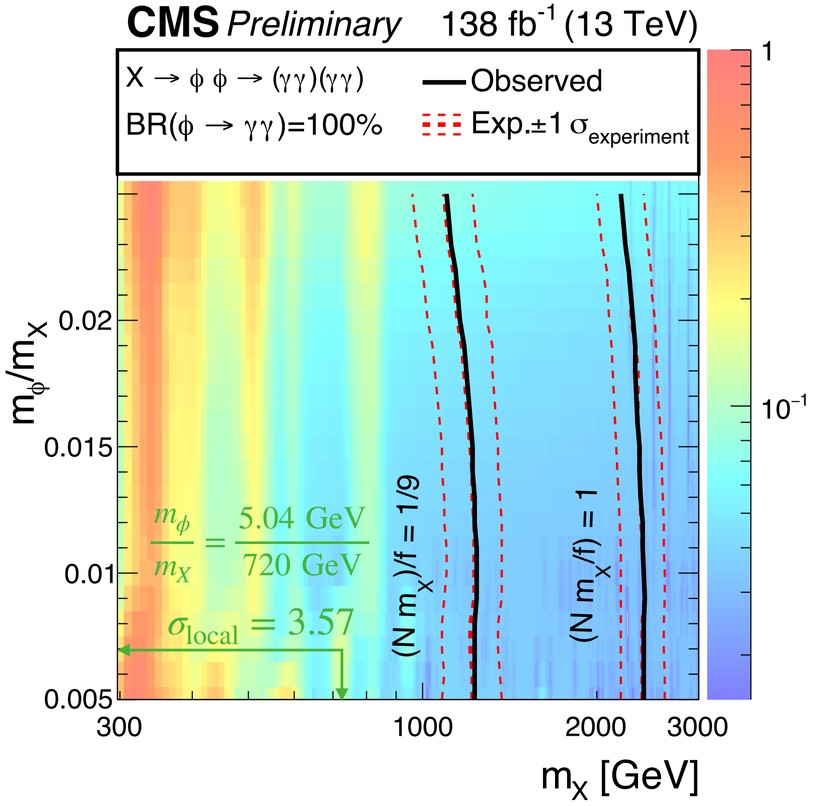

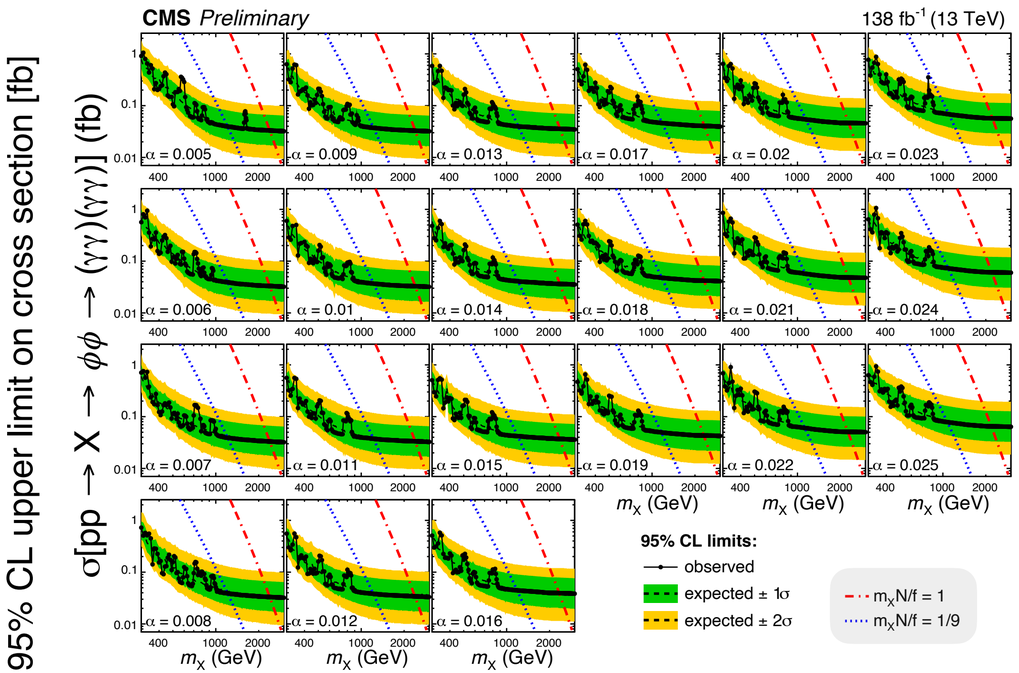

Cross section limit vs m_X for specific values of α

4 Leptons+MET/jets 2401.04742

- 2HDM and 2HDM+S models with
  - $S \rightarrow$ invisible (could be DM portal),
  - Fix $m_S = 160$ GeV to reduce free parameters (J. Phys. G 45 (2018) 115003)
  - $320(390) < m_{A(R)} < 1300$ GeV and $220 < m_H < 1000$ GeV

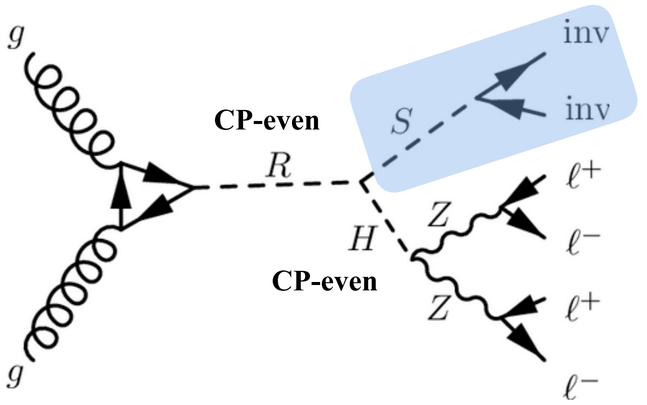

- Analysis is classified by 4μ, $4e$ and $2\mu 2e$, where $m_{4\ell} > 200$ GeV
  - Further divided into $N_{\text{jets}} = 0$ and > 0
  - $A \rightarrow ZH$ channel also categorized using $N_{b-\text{jets}}$
  - Altogether 7 signal regions
- Objects selection is std except for the vertex fit of the 4ℓ ID tracks
  - the $\chi^2/N_{\text{DoF}} < 9(6)$ requirement for 4μ (otherwise)
- Backgrounds are modeled with a function in MC, normalized to data
  - main source is $q\bar{q}(gg) \rightarrow ZZ$

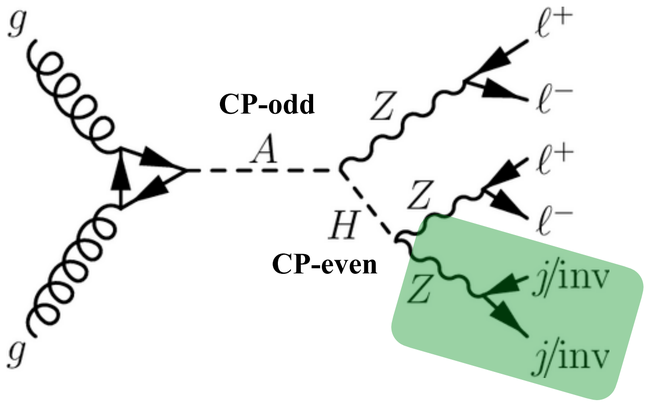

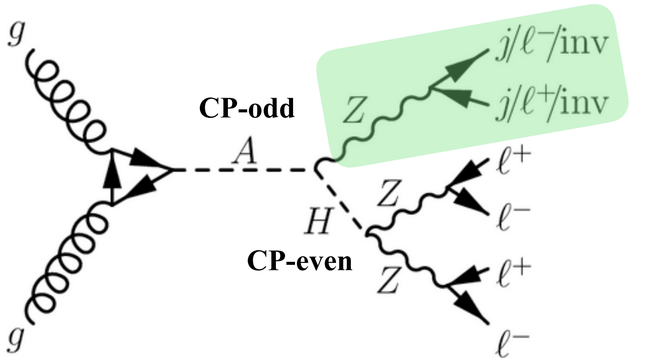

4 Leptons+MET/jets 2401.04742

- Search is dominated by statistical uncertainties
  - Impact of systematics on the fitted σ values is $\Delta\sigma/\sigma < 10\,\%$
- Complements previous $A \to ZH$ searches
- $R \to SH$ extends the $(gg \to)H \to ZZ \to 4\ell$ inclusive analysis

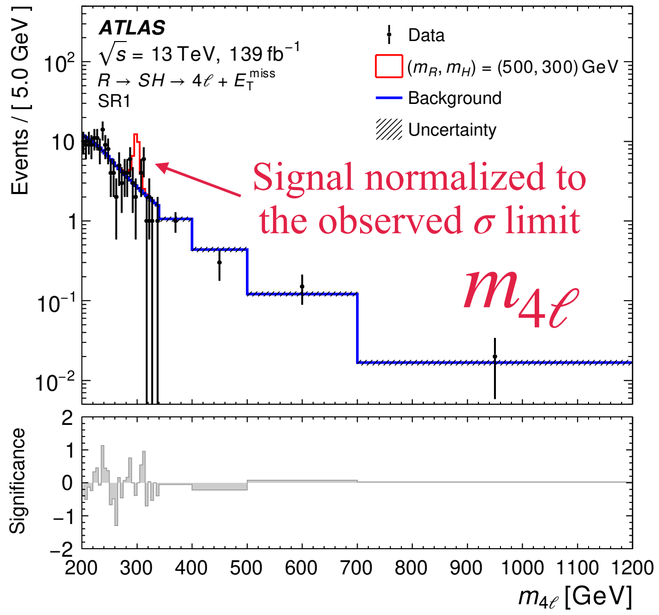

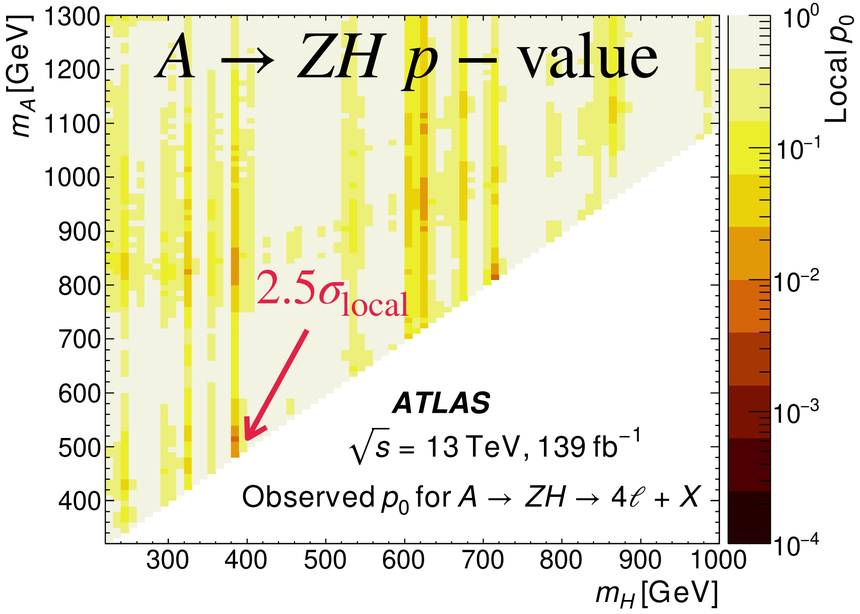

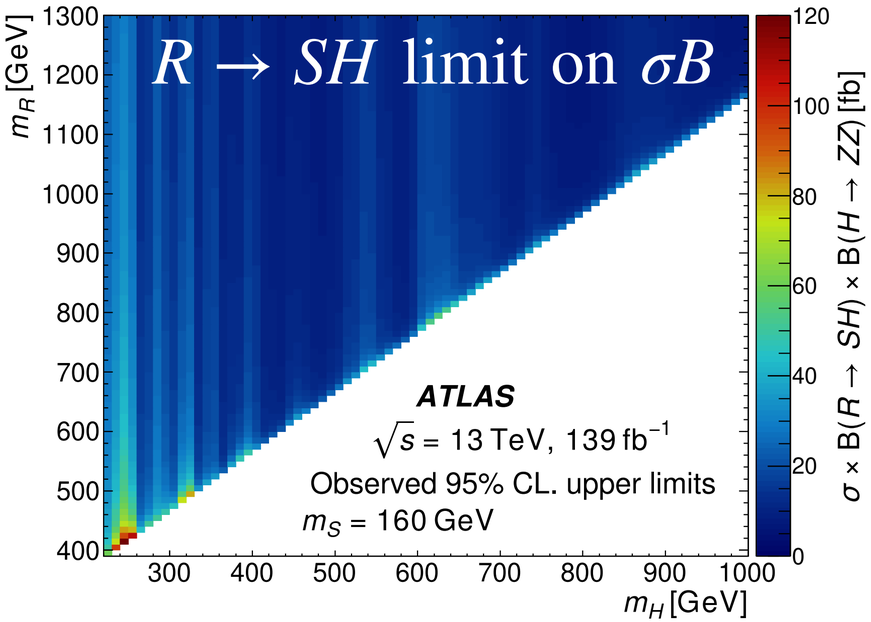

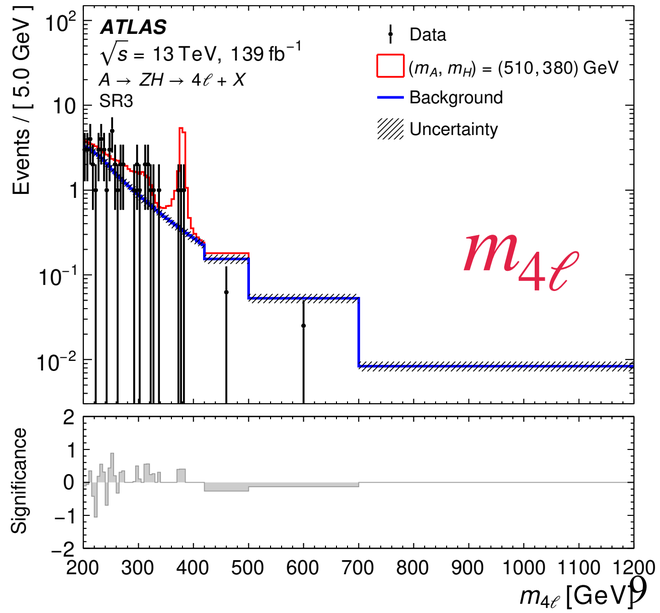

Narrow trijet resonances 2310.14023

- Benchmarks:
  - Right-handed Z boson, $Z_R \rightarrow 3g$
  - Excited quark $q^* \rightarrow qV_{BSM} \rightarrow 3q$
  - KK gluon $G_{KK} \rightarrow g\phi_{Radion} \rightarrow 3g$

$\Big\}\ X \rightarrow jY \rightarrow jjj$

$$0.2 < \rho_m \equiv \frac{m_Y}{m_X} < 0.8$$

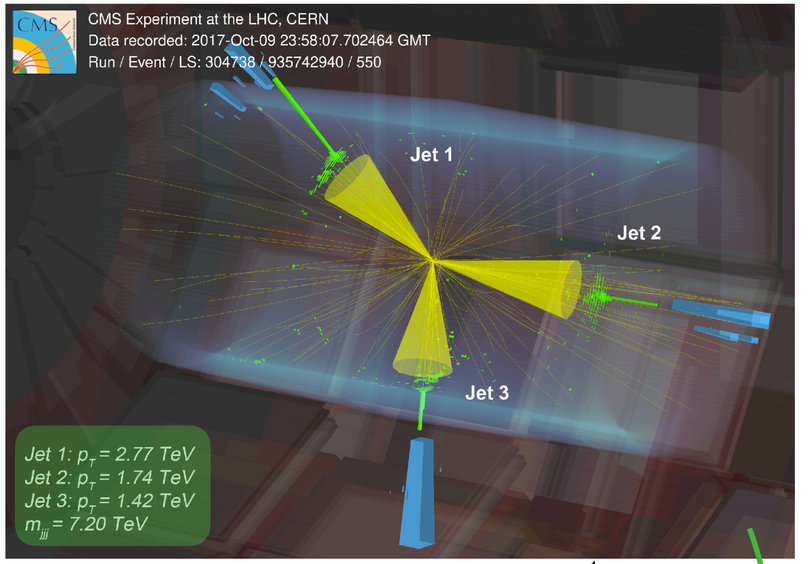

- Search for an excess in m_{jjj} with 3 resolved "wide jets" (Phys. Lett. B 704 (2011) 123)
  - Wide jet: take the 3 leading jets with $p_T > 100$ GeV as seeds and add any jet with $p_T > 30$ GeV if $\Delta R < 1.1$ (recover QCD radiation outside the jet)
  - Extending the semi-resolved search (intermediate particle is boosted)
  - $m_{jjj} > 1.50$ (1.76) TeV for 2016 (2017-2018) due to jet/H_T triggers

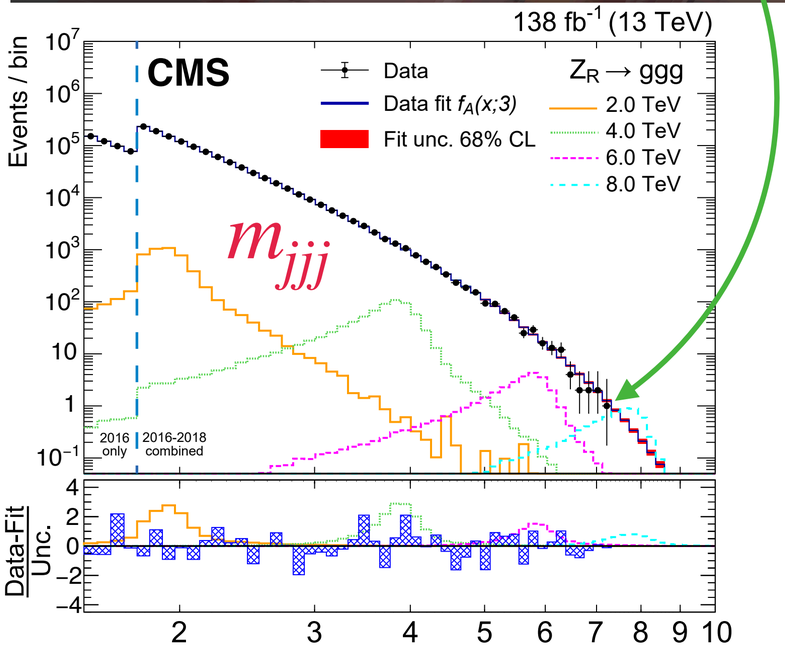

- Background is QCD multijet only, estimated from a fit to the data
  - Uncertainties: alternative functions and fit parameters

Narrow trijet resonances 2310.14023

- Jet energy resolution uncertainty translates to ~10% uncertainty in the m_{jjj} shape width
- Dominant uncertainties: bkg fit parameters (impact the fitted signal strength by ~10%)

Direct or cascade decays, for specific values of $\rho_m = \frac{m_Y}{m_X}$

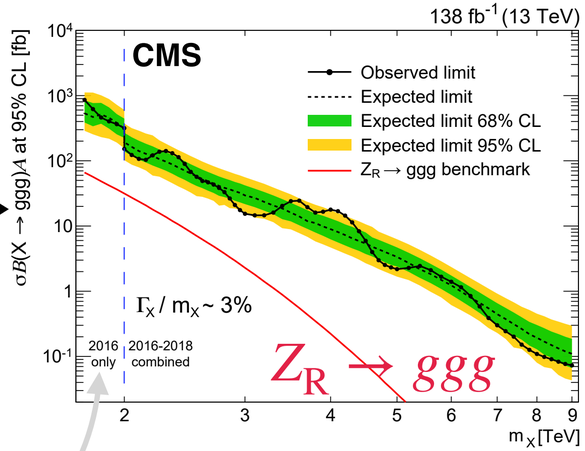

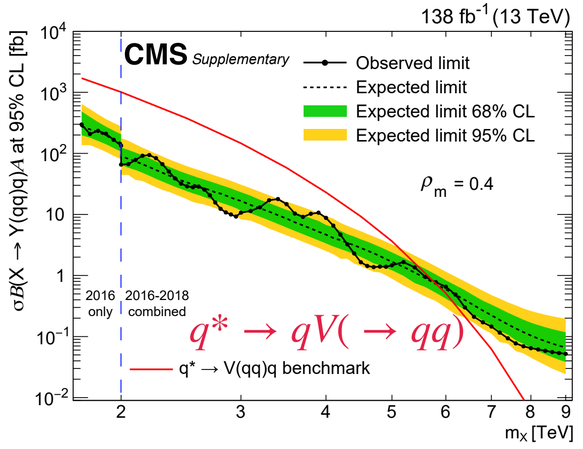

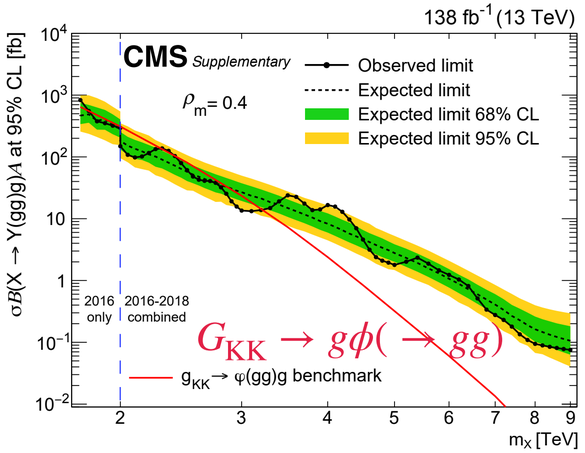

Only the 2016 data are used to derive limits below 2.0 TeV because of the higher trigger thresholds in 2017-2018

Cascade decays with $\rho_m = \frac{m_Y}{m_X}$ versus m_X

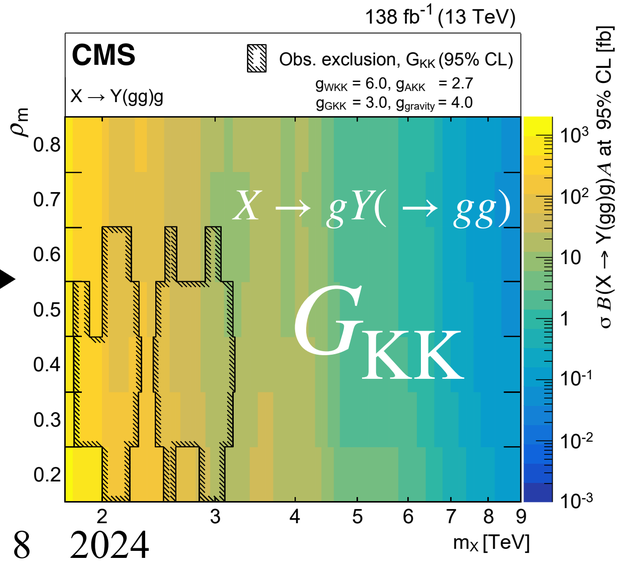

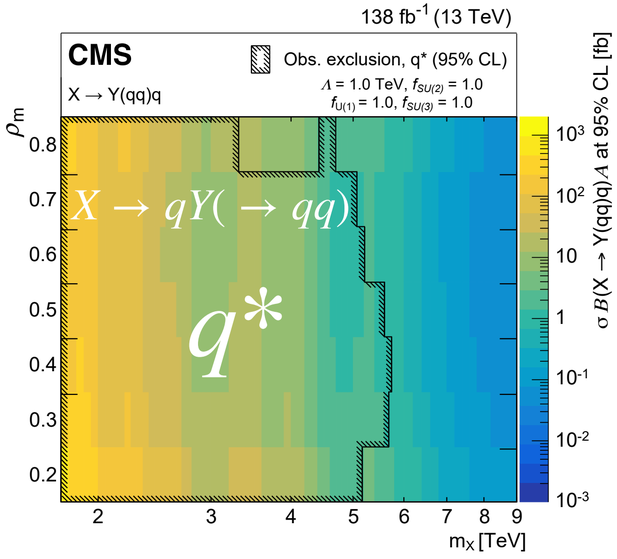

Heavy resonances combination 2402.10607

- Spin-1 $X \to VV/hh/qq/\ell\ell$
  - Remove small overlaps between analyses if any
  - Including for the first time final states like $qq, bb, t\bar{t}, tb, \tau\nu, \tau\tau$

$$\mathcal{L}_{\mathcal{W}}^{\text{int}} = -g_q \mathcal{W}_\mu^a \bar{q}_k \gamma^\mu \frac{\sigma_a}{2} q_k - g_\ell \mathcal{W}_\mu^a \bar{\ell}_k \gamma^\mu \frac{\sigma_a}{2} \ell_k - g_H \left(\mathcal{W}_\mu^a H^\dagger \frac{\sigma_a}{2} i D^\mu H + \text{h.c.} \right)$$

- Looking at spin-1 heavy vector triplet (HVT) framework:
  - iso-triplet $\mathscr{W}$ of colorless vector bosons with zero hypercharge
  - nearly degenerate charged, $W'^{\pm}$, and neutral, Z'
  - allows to explore different $V/h/q/\ell$ couplings strengths

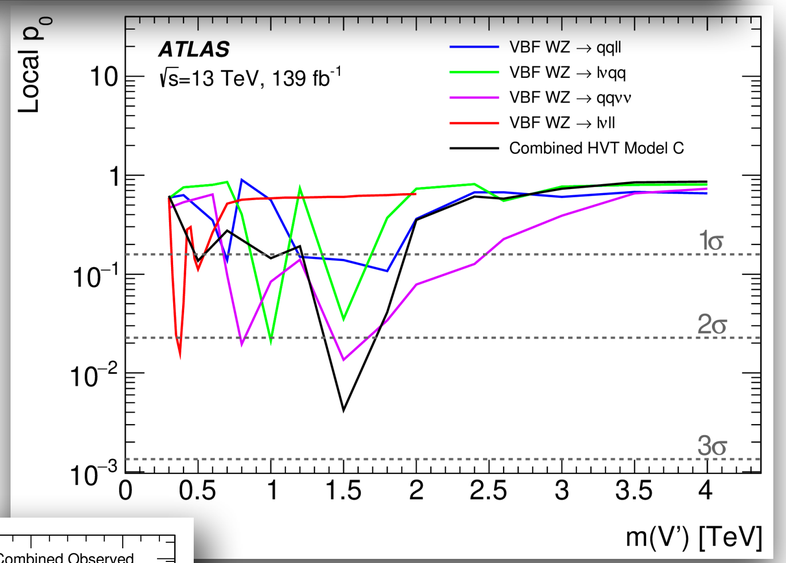

- Systematics weaken the limit on $\sigma(pp \to V')$ by <20%,
- Modest excess around $m = 1.5$ TeV with $\sigma_{\text{local}} = 2.6$
  - driven by the $qq\nu\nu$, $\ell\nu qq$, and $qq\ell\ell$ VBF channels

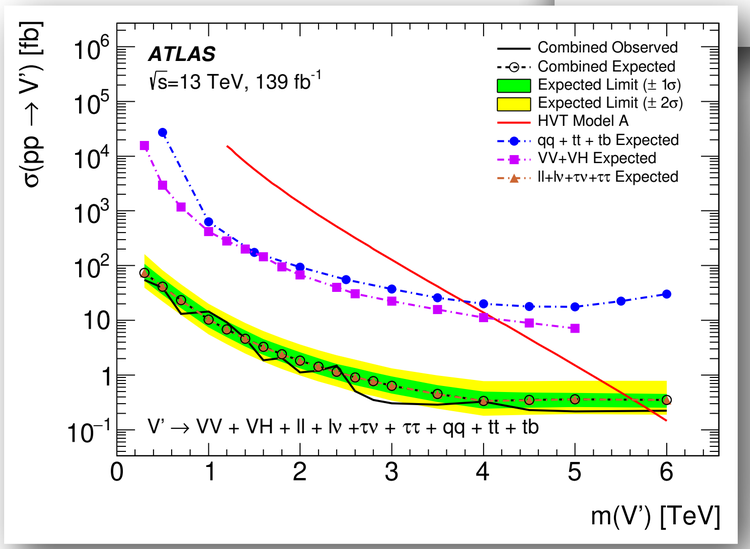

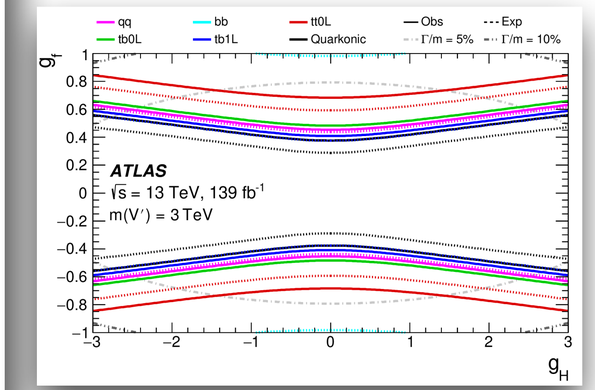

- Check paper to see the full 2D exclusion limits
  - Bosonic, Leptonic and Quarkonic subcombination
  - Full combination

Resonant HH combination 2311.15956

- $b\bar{b}b\bar{b}$: **33.9%, most sensitive at high masses**
  - Resolved: BDT is used to pair the *b*-jets to form the HH
  - Boosted: 2/3/4 b-tagged track-jets associated with each of the 2 large-R jets
- $b\bar{b}\tau^+\tau^-$: **7.3%, most sensitive in intermediate masses**
  - Only had-had and had-lep
  - Score of a mass-parameterized NN used as an observable
- $b\bar{b}\gamma\gamma$: **0.3%, most sensitive at low masses**
  - Diphoton mass is constrained to the Higgs mass
  - BDT to discriminate between signal and background

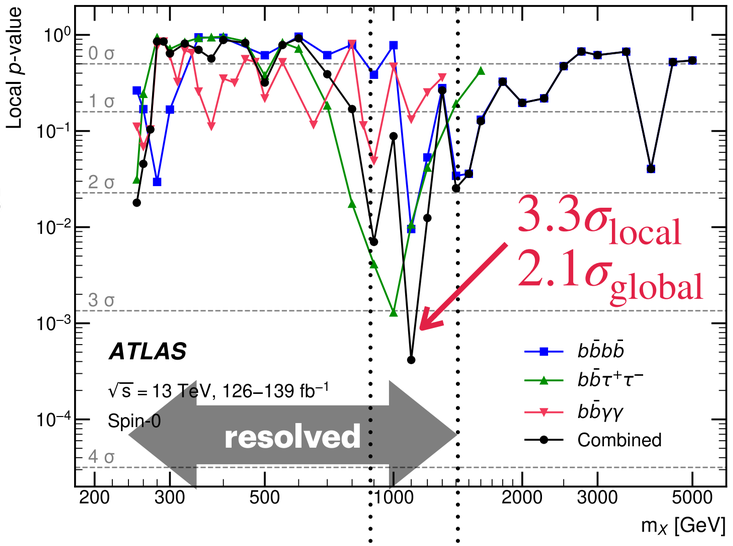

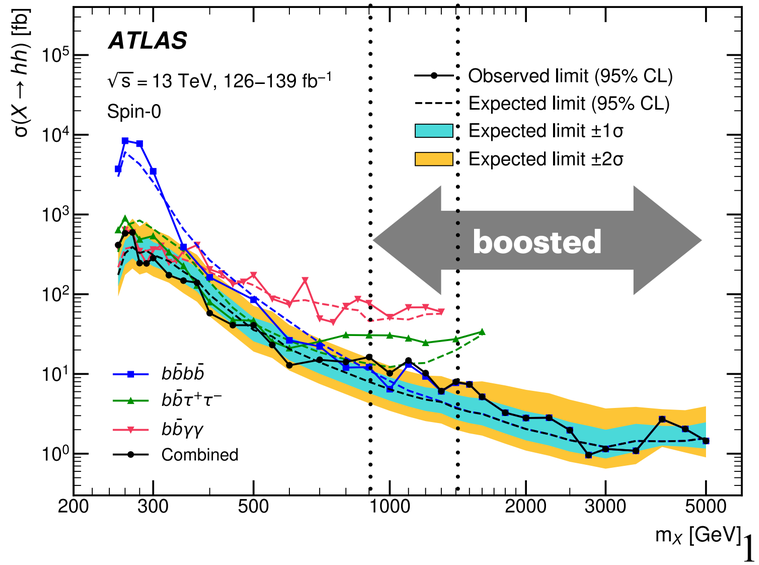

- b-jets identification: DL1r@77% (new graph NN taggers are coming!)
- Uncertainties impact on the combined limit is ~3-10%
- Limits improve by a factor 1-5 wrt the previous ATLAS combination
- Check paper to see more limits on Type-1 2HDM and MSSM

Outlook

- This was only a tiny fraction of ATLAS and CMS's search efforts
- More in the pipeline for Run 2, and many more will come after Run 3
  - maybe discovery(ies?), but surely can expect many combinations
  - watch for scenarios which benefit from the cross-section increase in $\sqrt{s}$
- Turn every stone, but recall: past discoveries were made mostly via fermionic decays

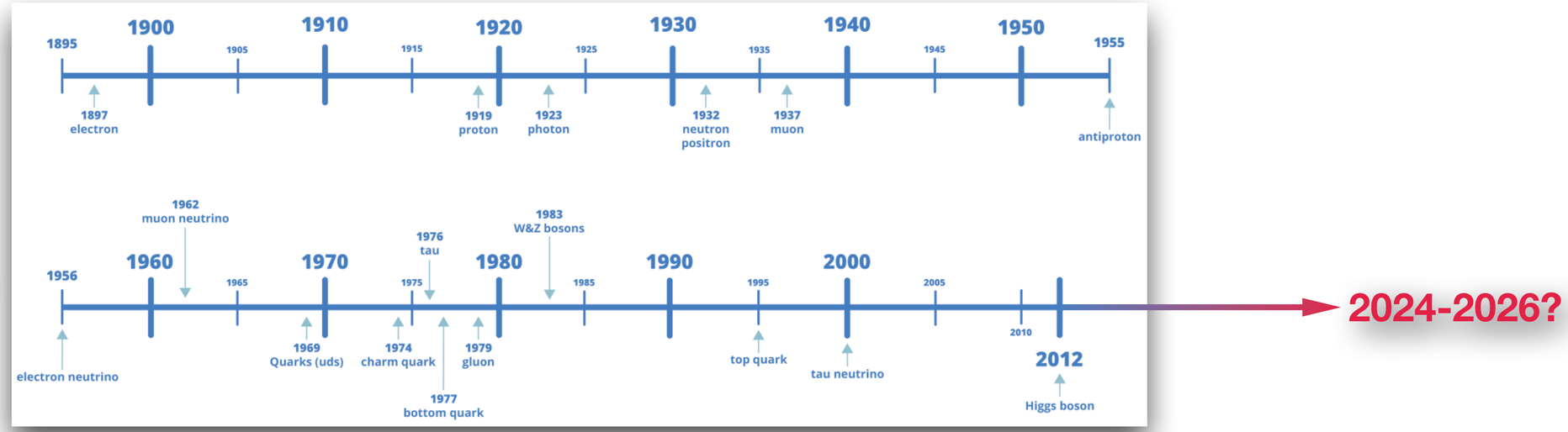


THANK YOU

BACKUP

Tau+MET

	Preselection
$E_{\mathrm{T}}^{\mathrm{miss}}$ trigger	70, 90, 110 GeV
Event cleaning	applied
$\tau_{\text{had-vis}}$ tracks	1 or 3
$\tau_{\text{had-vis}}$ charge	± 1
$\tau_{\text{had-vis}}$ p_{T}	> 30 GeV
$\tau_{\text{had-vis}}$ $p_{\mathrm{T}}^{\mathrm{leadTrack}}$	> 10 GeV
Lepton veto	applied
$\Delta\phi(\tau_{\text{had-vis}} p_{\mathrm{T}}, E_{\mathrm{T}}^{\mathrm{miss}})$	> 2.4 rad

	Region requirements				
	SR	**CR1**	**CR2**	**CR3**	**VR**
Tau identification	L	VL \ L	L	VL \ L	L
$E_{\mathrm{T}}^{\mathrm{miss}}$	> 150 GeV	> 150 GeV	< 100 GeV	< 100 GeV	> 150 GeV
$p_{\mathrm{T}}/E_{\mathrm{T}}^{\mathrm{miss}}$	$\in [0.7, 1.3]$	$\in [0.7, 1.3]$	–	–	< 0.7
m_{T}	–	–	–	–	> 240 GeV

Table 3: Summary of the event selection. The top part of the table summarizes the "preselection" requirements that apply to all regions used in this analysis. The bottom part shows the additional selection requirements for each individual region. Here, the symbol L stands for *loose* tau identification and VL\L denotes the requirement that the tau candidate must pass the *very loose* but fail the *loose* identification.

Tau+MET

Selection	Data	$W \to \tau\nu$	Jet background	Other background	W'_{SSM} (5 TeV)
Preselection	3640749	101810	–	73171	18.463
Tau identification	1189863	84370	–	52482	16.804
$E_{\mathrm{T}}^{\mathrm{miss}} > 150$ GeV	58528	13406	30760	11953	15.090
$0.7 < \frac{p_{\mathrm{T}}}{E_{\mathrm{T}}^{\mathrm{miss}}} < 1.3$	18528	9662	5761	2949	13.810
$m_{\mathrm{T}} > 1$ TeV	58	51.1	9.96	12.0	7.236

Table 2: Overview of the selected numbers of events, for the SM backgrounds and a W'_{SSM} signal of mass 5 TeV. The jet background is estimated from data and cannot be quantified before the requirements of $E_{\mathrm{T}}^{\mathrm{miss}} > 150$ GeV and tau identification. "Preselection" denotes all selection criteria described in Section 4 except for the tau identification, $E_{\mathrm{T}}^{\mathrm{miss}}$ and $p_{\mathrm{T}}/E_{\mathrm{T}}^{\mathrm{miss}}$ requirements. The last row summarizes the number of observed and expected events above a large m_{T} threshold, but is not part of the SR selection.

$$N_{\mathrm{SR}}^{\mathrm{jet}} = \sum_{i,j} (N_{\mathrm{CR1,ij}}^{\mathrm{data}} - N_{\mathrm{CR1,ij}}^{\mathrm{lepton}}) F_{ij} \quad \text{, where } F_{ij} = \frac{N_{\mathrm{CR2,ij}}^{\mathrm{data}} - N_{\mathrm{CR2,ij}}^{\mathrm{lepton}}}{N_{\mathrm{CR3,ij}}^{\mathrm{data}} - N_{\mathrm{CR3,ij}}^{\mathrm{lepton}}}$$

Tau+MET

Systematic uncertainty	Relative uncertainty on the jet background (%)	
	$200 < m_T < 300$ GeV	$m_T > 2000$ GeV
Non-jet background subtraction	+2.4/-3.3	+1.5/-16.5
Variation of E_T^{miss} thresholds	± 2.1	± 16.4
Quark/gluon ratio differences	± 3.2	± 12.7
Extrapolation of transfer factor	±2.3	±16.1
Alternative fit function	0	± 58
Lower fit range ±50 GeV	0	± 19
Higher fit range ±50 GeV	0	± 1.9
m_T rebinning	0	± 2.4

Table 4: Summary of the uncertainties on the jet background estimate.

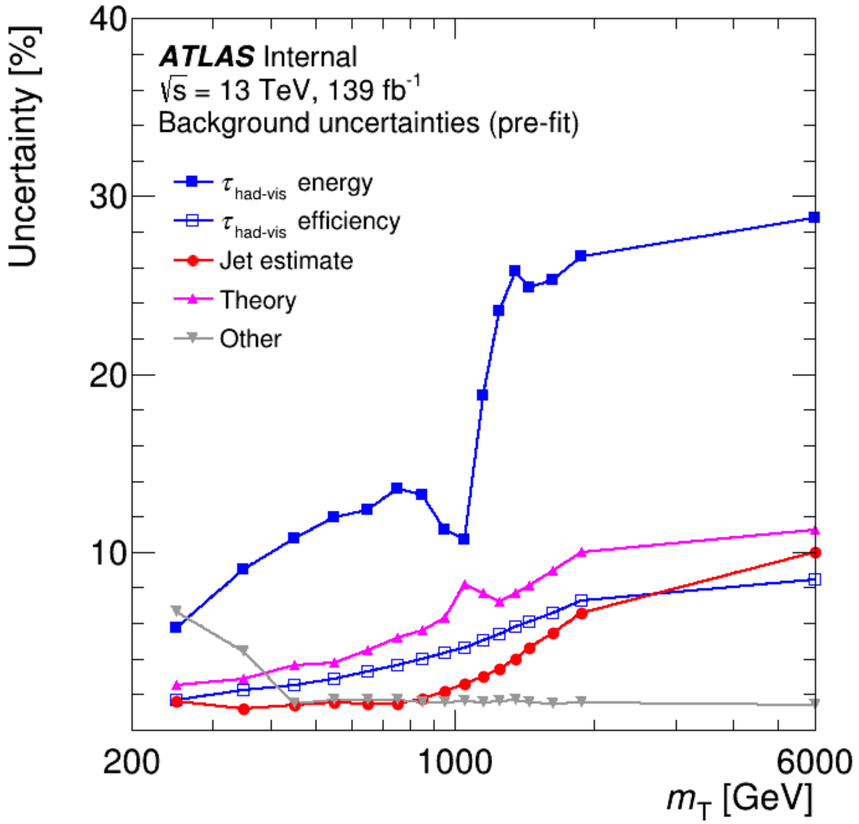

Merged diphotons

- For both CNNs the inputs are the individual crystal energies of that Γ, normalized such that the sum of all crystal energies is unity.
- Architecture of CNN_1 used for classification. The network takes in a pixelated image of a candidate cluster made from ECAL energy deposits, where each pixel is exactly one ECAL crystal. The output is fed through a fully connected linear network which gives three output scores corresponding to the likelihood of the cluster being a single photon, diphoton, or hadron.
- Architecture of CNN_2 used for diphoton m/E regression. The network takes in a pixelated image of a diphoton cluster as selected by the classification neural network. The output is fed through three fully connected linear networks which give the final m/E of the diphoton.
- In addition, the geometric η of the Γ is added as an additional input to the first FC layer
- The training of the classification neural network uses 600k total events, divided equally between the diphoton, single photon, and hadron categories. For the regression, 500k diphoton simulated events are used. In both cases, diphoton events are sampled to retain a flat m/E spectrum.

$CNN_1 \longrightarrow$ probabilities : $P_{\gamma\gamma}$, P_{γ}, P_{had}

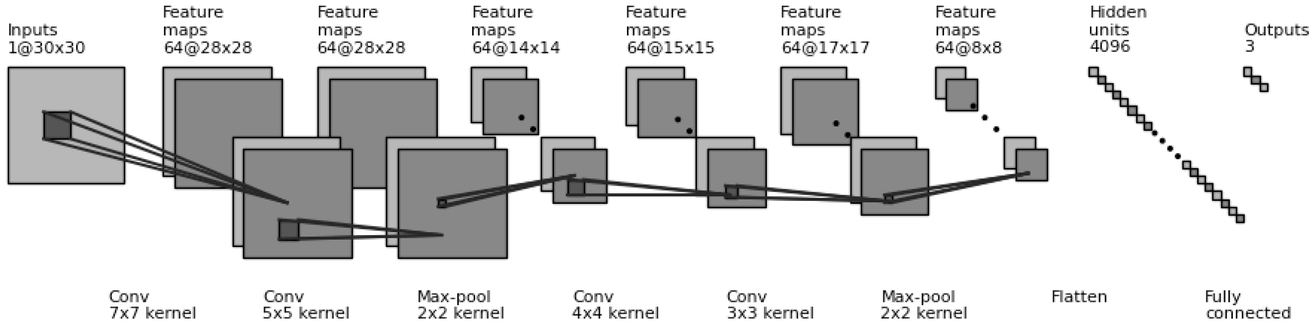

$CNN_2 \longrightarrow$ predict m/E

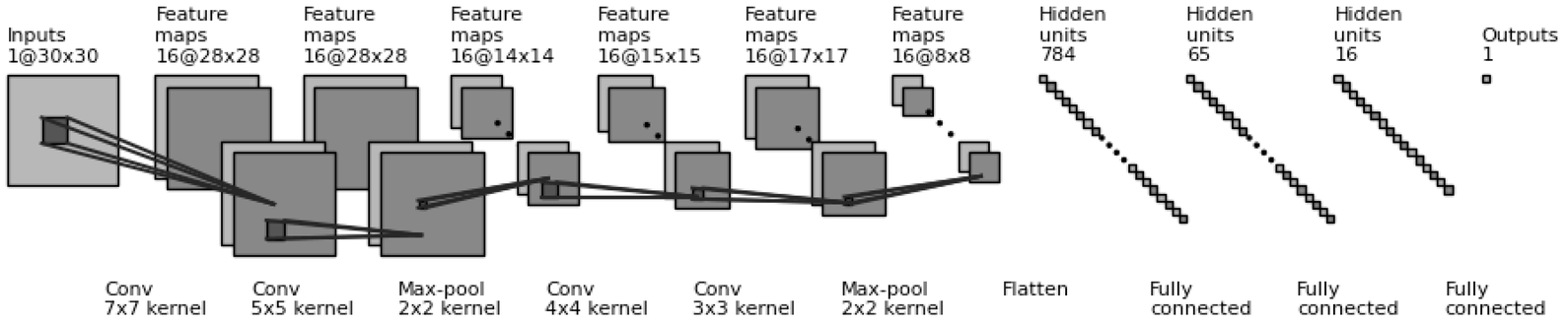

Merged diphotons

- If a Γ overlaps such a jet within $\Delta R \leq 0.15$, its r_{iso} is defined as the ratio of its energy to that of the jet. Otherwise, it is set to unity.
- Consider events with two Γs with $p_T > 90$ GeV, where the trigger becomes fully efficient. Only events in which both candidates deposit all their energy in the ECAL barrel ($|\eta| < 1.4$) are considered.
- Both Γs in the events are further required to fulfill the following requirements: riso > 0.8 and $P\gamma\gamma > 0.9$. Finally, the mass asymmetry of the event $m_{asym} = |m_{\Gamma 1} - m_{\Gamma 2}|/(m_{\Gamma 1} + m_{\Gamma 2})$ is required to be less than 0.25, and the separation in η between the two Γs is required to be greater than 1.5 to further suppress background from SM production of jets and photons.
- The remaining data is evaluated for localized excesses in the $m_{\Gamma\Gamma}$ distribution, in nine orthogonal divisions of the α_{reco} distributions ranging from 0.3% to 3%, determined by a combination of detector resolution and a requirement that each division contain enough events for the background estimate to converge.
- Any particular signal is expected to appear in only a few adjacent α_{reco} divisions

4l+MET/jets

Signal region	$R \to SH \to 4\ell + E_{\mathrm{T}}^{\mathrm{miss}}$ and $A \to ZH \to 4\ell + X$			
SR1	$n_{b\text{-jets}} = 0$	$n_{\mathrm{jets}} = 0$	$p_{\mathrm{T}}^{4\ell} > 20$ GeV	$E_{\mathrm{T}}^{\mathrm{miss}}$ significance >2.0
SR2		$n_{\mathrm{jets}} \geq 1$	$p_{\mathrm{T}}^{4\ell} > 10$ GeV	$E_{\mathrm{T}}^{\mathrm{miss}}$ significance > 3.5
SR3			$p_{\mathrm{T}}^{4\ell} < 10$ GeV	$2.5 < E_{\mathrm{T}}^{\mathrm{miss}}$ significance < 3.5
	$A \to ZH \to 4\ell + X$			
SR4	$n_{b\text{-jets}} = 0$	$n_{\mathrm{jets}} \geq 2$	$\lvert m_{jj} - m_Z \rvert < 20$ GeV	
SR5			$\lvert m_{jj} - m_Z \rvert > 20$ GeV	
SR6		$n_{\mathrm{jets}} = 1$		
SR7	$n_{b\text{-jets}} \geq 1$			

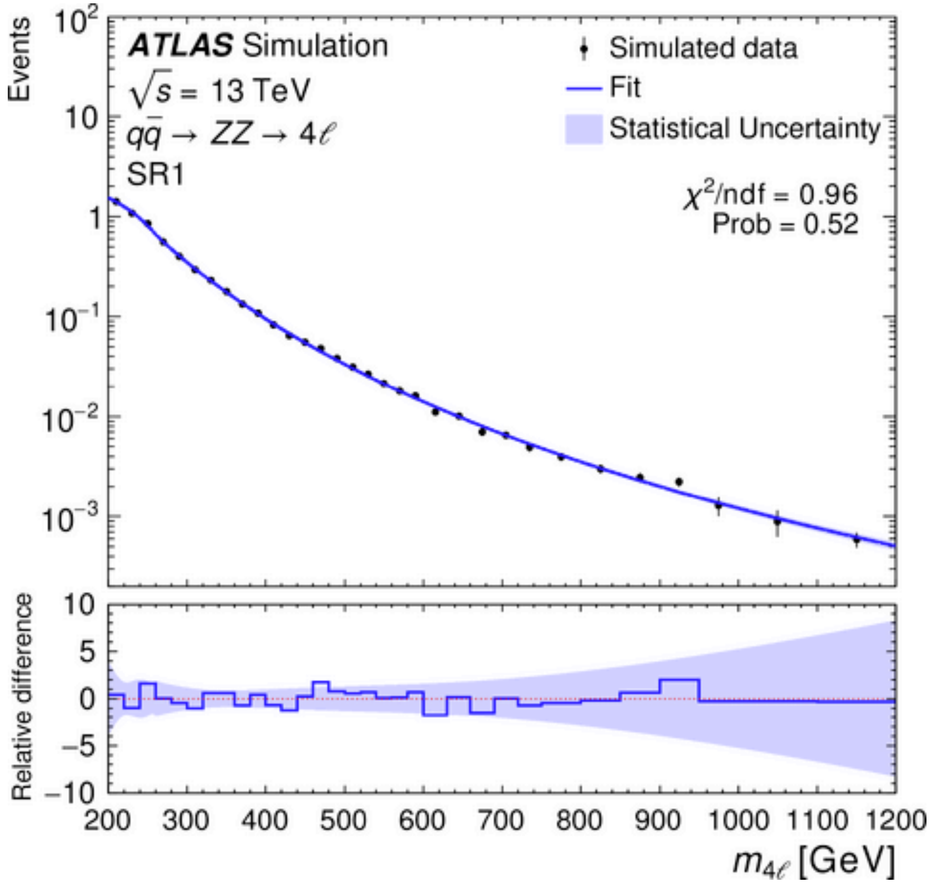

$$f(m_{4\ell}) = H(m_0 - m_{4\ell}) f_1(m_{4\ell})\, C_1 + H(m_{4\ell} - m_0) f_2(m_{4\ell})\, C_2, \tag{1}$$

where:

$$f_1(m_{4\ell}) = \frac{a_1 \cdot m_{4\ell} + a_2 \cdot m_{4\ell}^2}{1 + \exp\left(\frac{m_{4\ell} - a_1}{a_3}\right)}, \tag{2}$$

$$f_2(m_{4\ell}) = \left(1 - \frac{m_{4\ell}}{n_C}\right)^{b_1} \cdot \left(\frac{m_{4\ell}}{n_C}\right)^{\left(b_2 + b_3 \cdot \ln\left(\frac{m_{4\ell}}{n_C}\right)\right)}, \tag{3}$$

$$C_1 = \frac{1}{f_1(m_0)}, \qquad C_2 = \frac{1}{f_2(m_0)}.$$

The functional form f_1 models the ZZ threshold around $2 \cdot m_Z$, and f_2 describes the high mass tail. The transition between the f_1 and f_2 functions is performed by the Heaviside step function $H(x)$ around m_0, where m_0 is fixed to 260 GeV, 240 GeV, 250 GeV and 230 GeV for the $q\bar{q} \to ZZ$, $gg \to ZZ$, VVV, and other backgrounds, respectively. The transition point is determined by the smoothness of the functional

4l+MET/jets

Signal region	$R \to SH \to 4\ell + E_{\mathrm{T}}^{\mathrm{miss}}$ and $A \to ZH \to 4\ell + X$			
SR1	$n_{b\text{-jets}} = 0$	$n_{\mathrm{jets}} = 0$	$p_{\mathrm{T}}^{4\ell} > 20$ GeV	$E_{\mathrm{T}}^{\mathrm{miss}}$ significance >2.0
SR2		$n_{\mathrm{jets}} \geq 1$	$p_{\mathrm{T}}^{4\ell} > 10$ GeV	$E_{\mathrm{T}}^{\mathrm{miss}}$ significance > 3.5
SR3			$p_{\mathrm{T}}^{4\ell} < 10$ GeV	$2.5 < E_{\mathrm{T}}^{\mathrm{miss}}$ significance < 3.5
	$A \to ZH \to 4\ell + X$			
SR4	$n_{b\text{-jets}} = 0$	$n_{\mathrm{jets}} \geq 2$	$\lvert m_{jj} - m_Z \rvert < 20$ GeV	
SR5			$\lvert m_{jj} - m_Z \rvert > 20$ GeV	
SR6		$n_{\mathrm{jets}} = 1$		
SR7	$n_{b\text{-jets}} \geq 1$			

	SR1	SR2	SR3	SR4	SR5	SR6	SR7
$q\bar{q} \to ZZ$	132 ± 12	17 ± 6	42 ± 7	40 ± 7	156 ± 13	549 ± 70	86 ± 11
$gg \to ZZ$	32 ± 6	3.2 ± 3.1	8.3 ± 3.1	6.6 ± 2.8	22.1 ± 3.7	102 ± 70	9.4 ± 4.2
VVV	7.5 ± 0.4	4.77 ± 0.34	1.49 ± 0.19	0.19 ± 0.04	1.08 ± 0.11	1.59 ± 0.13	0.50 ± 0.07
Other backgrounds	5.5 ± 0.9	7.1 ± 1.1	3.6 ± 0.7	2.47 ± 0.30	17.5 ± 0.8	11.3 ± 0.8	37.6 ± 2.3
Total background	177 ± 13	32 ± 6	55 ± 7	49 ± 7	197 ± 14	664 ± 26	134 ± 12
Observed	177	32	55	49	197	664	135
μ_{norm}^{ZZ}	1.15 ± 0.15	1.3 ± 0.6	0.96 ± 0.22	0.90 ± 0.17	0.80 ± 0.08	1.02 ± 0.13	1.4 ± 0.3

Table 3: Observed and expected post-fit event yields for $m_{4\ell} > 200$ GeV with their uncertainties. The expected yields and their uncertainties are obtained from a simultaneous fit to data under the background-only hypothesis on all seven signal regions discussed in Section 5. The μ_{norm}^{ZZ} is the normalisation factor for the $q\bar{q} \to ZZ$ and $gg \to ZZ$ backgrounds. The other backgrounds include $q\bar{q} \to ZZ$ (EW), $t\bar{t}V$, $t\bar{t}$, Z+jets and WZ processes. These backgrounds and the VVV background process were fixed to their SM prediction.

4l+MET/jets

$R \to SH \to 4\ell + E_{\mathrm{T}}^{\mathrm{miss}}$			$A \to ZH \to 4\ell + X$		
(m_R, m_H) [GeV]	Uncertainty source	$\Delta\sigma/\sigma$ [%]	(m_A, m_H) [GeV]	Uncertainty source	$\Delta\sigma/\sigma$ [%]
(390, 220)	Jet flavour composition	6.2	(320, 220)	Other backgrounds parameterisation SR7	5.0
	Jet flavour response	4.8		$q\bar{q} \to ZZ$ parameterisation SR7	3.9
	Jet energy scale	4.2		Jet flavour composition	3.9
	Pile-up reweighting	4.0		Luminosity	3.7
	CKKW parton showering ($gg \to ZZ$) SR2	3.8		$gg \to ZZ$ parameterisation SR6	3.6
(500, 300)	CKKW parton showering ($gg \to ZZ$) SR2	3.1	(510, 380)	Luminosity	2.4
	QSF parton showering ($gg \to ZZ$) SR2	3.0		Jet flavour composition	2.4
	$q\bar{q} \to ZZ$ parameterisation SR2	2.0		Jet energy scale	1.7
	Pile-up reweighting	1.9		Jet energy resolution	1.5
	VVV parameterisation SR2	1.9		Signal PDF	1.4
(1300, 1000)	$q\bar{q} \to ZZ$ parameterisation SR2	9.3	(1300, 1000)	CKKW parton showering ($gg \to ZZ$) SR2	3.3
	Jet flavour composition	7.3		QSF parton showering ($gg \to ZZ$) SR2	3.3
	Jet flavour response	3.5		Other backgrounds parameterisation SR2	2.6
	Pile-up reweighting	2.9		$q\bar{q} \to ZZ$ parameterisation SR5	2.1
	CKKW parton showering ($gg \to ZZ$) SR2	2.9		VVV parameterisation SR2	2.1

Table 4: The impact of the most important sources of uncertainty on the best-fit value of the signal cross-section for three mass points for each $R \to SH \to 4\ell + E_{\mathrm{T}}^{\mathrm{miss}}$ and $A \to ZH \to 4\ell + X$ signals after the fit. Sum in quadrature of the upward and downward effects ($\Delta\sigma$) is divided by the best fit value of the signal cross-section (σ) for each signal. Shape uncertainties are uncorrelated and hence affect each region separately.

4l+MET/jets

Width assumptions	Mass points [GeV]	Upper limits in the $\sigma(gg \to A)$ [fb]		Ratio w.r.t Narrow width
		Observed	Expected	
Narrow width	$(m_A, m_H) = (320, 220)$	19.6	25.1	1.0
	$(m_A, m_H) = (1190, 600)$	4.8	3.5	1.0
$(\Gamma_A/m_A, \Gamma_H/m_H) = (15\%, 5\%)$	$(m_A, m_H) = (320, 220)$	31.5	36.2	1.4
	$(m_A, m_H) = (1190, 600)$	8.3	6.0	1.7
$(\Gamma_A/m_A, \Gamma_H/m_H) = (30\%, 10\%)$	$(m_A, m_H) = (320, 220)$	38.9	42.5	1.7
	$(m_A, m_H) = (1190, 600)$	8.9	6.6	1.9

Table 5: Observed and expected upper limits at 95% confidence level (CL) on the $\sigma(gg \to A) \times \mathcal{B}(A \to ZH) \times \mathcal{B}(H \to ZZ)$ for different large width approximation signals for comparison with the narrow width approximation. The fraction in the rightmost column corresponds to the ratio between the expected upper limits with large- or narrow width signals. The Γ_A and Γ_H denote the widths of the A and H bosons, respectively.

4l+MET/jets

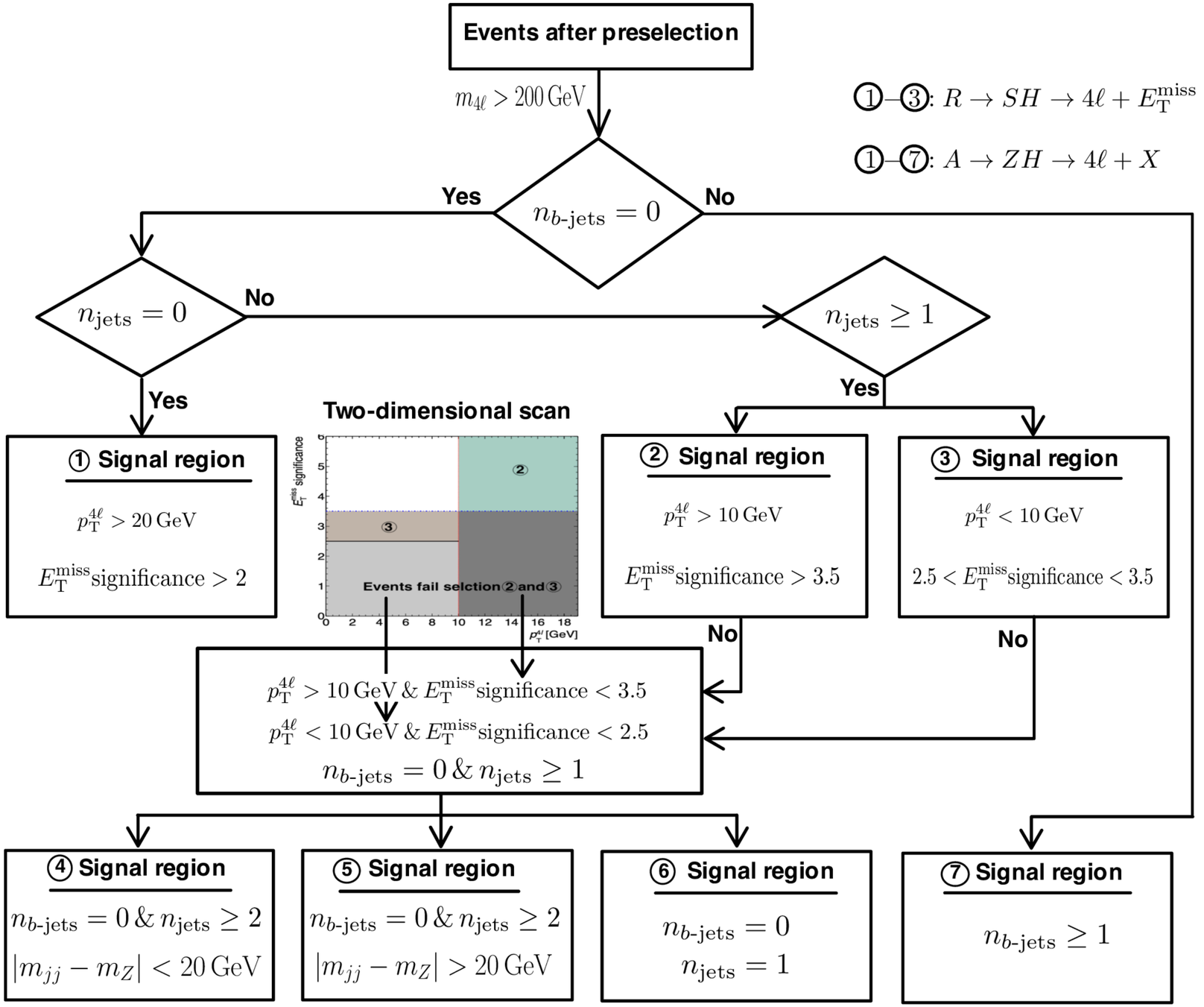
Events after preselection
$m_{4\ell} > 200\,\text{GeV}$
①–③: $R \to SH \to 4\ell + E_{\text{T}}^{\text{miss}}$
①–⑦: $A \to ZH \to 4\ell + X$
$n_{b\text{-jets}} = 0$
Yes
No
$n_{\text{jets}} = 0$
No
$n_{\text{jets}} \geq 1$
Yes
Yes
Two-dimensional scan
$E_{\text{T}}^{\text{miss}}$ significance
$p_{\text{T}}^{4\ell}$ [GeV]
Events fail selction ② and ③
① Signal region
$p_{\text{T}}^{4\ell} > 20\,\text{GeV}$
$E_{\text{T}}^{\text{miss}}$significance > 2
② Signal region
$p_{\text{T}}^{4\ell} > 10\,\text{GeV}$
$E_{\text{T}}^{\text{miss}}$significance > 3.5
③ Signal region
$p_{\text{T}}^{4\ell} < 10\,\text{GeV}$
$2.5 < E_{\text{T}}^{\text{miss}}$significance < 3.5
No
No
$p_{\text{T}}^{4\ell} > 10\,\text{GeV}$ & $E_{\text{T}}^{\text{miss}}$significance < 3.5
$p_{\text{T}}^{4\ell} < 10\,\text{GeV}$ & $E_{\text{T}}^{\text{miss}}$significance < 2.5
$n_{b\text{-jets}} = 0$ & $n_{\text{jets}} \geq 1$
④ Signal region
$n_{b\text{-jets}} = 0$ & $n_{\text{jets}} \geq 2$
$|m_{jj} - m_Z| < 20\,\text{GeV}$
⑤ Signal region
$n_{b\text{-jets}} = 0$ & $n_{\text{jets}} \geq 2$
$|m_{jj} - m_Z| > 20\,\text{GeV}$
⑥ Signal region
$n_{b\text{-jets}} = 0$
$n_{\text{jets}} = 1$
⑦ Signal region
$n_{b\text{-jets}} \geq 1$

Trijets

- Background shapes for $x \equiv m_{jjj}/\sqrt{s}$
- N is the order of the fit function, which is determined using a Fisher F-test.
  - It is found that the third order yields the best fits to the data for all three families of functions
-

$$f_A(x;\, N) = p_0 \frac{(1-x)^{p_1}}{x^{\sum_{i=2}^{N} p_i \log^{i-2}(x)}},$$

$$f_B(x;\, N) = p_0 \frac{\mathrm{e}^{-p_1 x}}{x^{\sum_{i=2}^{N} p_i \log^{i-2}(x)}},$$

$$f_C(x;\, N) = p_0 x^{\sum_{i=1}^{N} p_i \log^{i-1}(x)},$$

Heavy resonances combination

Table 1: Summary of event selection for the signal regions of the analyses used in the combination. The entries which are separated by commas denote an 'OR' of different signal regions. For jets, 'j' indicates a small-R jet, while 'J' denotes a large-R jet. The symbol $\subset$ denotes any combination of at least one of the objects inside the bracket up to the number shown. Entries denoted by a '-' indicate no requirement for that object. The VBF column indicates whether the analysis has an additional category for VBF events. The abbreviation 'Discr.' stands for the discriminating variable used in a given search.

Analysis	Leptons	$E_{\mathrm{T}}^{\mathrm{miss}}$	Jets	b-tags	Top-tags	VBF	Discr.	Reference
$WW/WZ \to qqqq$	0	Veto	≥2J	-	-	-	m_{VV}	[9]
$WW/WZ \to \ell\nu qq$	$1e$, 1μ	Yes	≥2j, ≥1J	0, 1, 2	-	Yes	m_{VV}	[10]
$WZ \to qq\nu\nu$	0	Yes	≥1J	0	-	Yes	m_{VV}	[10]
$WZ \to qq\ell\ell$	$2e$, 2μ	-	≥2j, ≥1J	0	-	Yes	m_{VV}	[10]
$WZ \to \ell\nu\ell\ell$	$3 \subset (e, \mu)$	Yes	-	0	-	Yes	m_{VV}	[11]
$WH/ZH \to qqbb$	0	Veto	≥2J	1, 2	-	-	m_{VH}	[12]
$ZH \to \nu\nu bb$	0	Yes	≥2j, ≥1J	1, 2	-	-	m_{VH}	[13]
$WH \to \ell\nu bb$	$1e$, 1μ	Yes	≥2j, ≥1J	1, 2	-	-	m_{VH}	[13]
$ZH \to \ell\ell bb$	$2e$, 2μ	Veto	≥2j, ≥1J	1, 2	-	-	m_{VH}	[13]
$\ell\nu$	$1e$, 1μ	Yes	-	-	-	-	m_{T}	[15]
$\tau\nu$	1τ	Yes	-	-	-	-	m_{T}	[16]
$\ell\ell$	≥$2e$, ≥2μ	-	-	-	-	-	$m_{\ell\ell}$	[14]
$\tau\tau$	0, $1e$, 1μ	Yes	-	0, ≥1	-	-	$m_{\tau\tau}$	[17]
tt0L	0	-	2J	1, 2	2	-	m_{tt}	[19]
tb0L	0	-	≥(1j+1J)	≥1	1	-	m_{tb}	[20]
tb1L	$1e$, 1μ	Yes	2j, 3j	1, 2	-	-	m_{tb}	[20]
qq	0	-	2j	0	-	-	m_{jj}	[18]
bb	0	-	2j	1, 2	-	-	m_{bb}	[18]